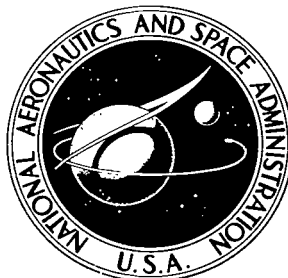


NASA TECHNICAL NOTE



NASA TN D-5846

C.1

NASA TN D-5846

TO: [illegible]
FROM: [illegible]
DATE: [illegible]

0132583



TECH LIBRARY KAFB, NM

CHARTS FOR ESTIMATING BOUNDARY-LAYER TRANSITION ON FLAT PLATES

*by Edward J. Hopkins, Don W. Jillie,
and Virginia L. Sorensen*

*Ames Research Center
Moffett Field, Calif. 94035*

NATIONAL AERONAUTICS AND SPACE ADMINISTRATION • WASHINGTON, D. C. • JUNE 1970





0132583

1. Report No. NASA TN D-5846	2. Government Accession No.	3. Recipient's Catalog No.	
4. Title and Subtitle CHARTS FOR ESTIMATING BOUNDARY-LAYER TRANSITION ON FLAT PLATES		5. Report Date June 1970	
		6. Performing Organization Code	
7. Author(s) Edward J. Hopkins, Don W. Jillie, and Virginia L. Sorensen		8. Performing Organization Report No. A-3370	
		10. Work Unit No. 129-01-20-03-00-21	
9. Performing Organization Name and Address NASA Ames Research Center Moffett Field, Calif. 94035		11. Contract or Grant No.	
		13. Type of Report and Period Covered Technical Note	
12. Sponsoring Agency Name and Address National Aeronautics and Space Administration Washington, D. C. 20546		14. Sponsoring Agency Code	
		15. Supplementary Notes	
16. Abstract Charts are presented for rapidly estimating the end of boundary-layer transition for flat plate wind-tunnel models with supersonic leading edges at an angle of attack of 0° . These charts were developed from the semiempirical method of Deem and Murphy who derived an equation that accounts for the combined effects of Mach number, unit Reynolds number, leading-edge sweep, leading-edge bluntness, and wall temperature on transition Reynolds number.			
17. Key Words (Suggested by Author(s)) Boundary-layer transition Unit Reynolds number Leading-edge sweep Leading-edge bluntness Mach number Wall temperature		18. Distribution Statement Unclassified - Unlimited	
19. Security Classif. (of this report) Unclassified	20. Security Classif. (of this page) Unclassified	21. No. of Pages 31	22. Price* \$ 3.00

NOTATION

b	leading-edge thickness
b_1	leading-edge thickness defined by equation (11) (see sketch (a))
b_2	leading-edge thickness defined by equation (12) (see sketch (a))
C_1	variable contained in equation (A1)
M_∞	free-stream Mach number
M_n	bluntness reduced Mach number (determined from the ratio of total pressure behind the shock at the leading edge and the free-stream static pressure)
R_b	bluntness Reynolds number, $(R/\text{inch})_\infty(b)$
R_t	transition Reynolds number, $(R/\text{inch})_\infty(x_t)$
$R_{t,o}$	transition Reynolds number for $b = 0$ as defined by equation (1)
$(R_{t,o})_n$	transition Reynolds number as defined by equation (3)
$R_{t,1}$	transition Reynolds number which accounts for both bluntness reduced Mach number and reduced unit Reynolds number effects, $(R_{t,o})_n \frac{(R/\text{inch})_\infty}{(R/\text{inch})_n}$
$R_{t,2}$	transition Reynolds number which accounts for only bluntness reduced unit Reynolds number effects, $(R_{t,o}) \frac{(R/\text{inch})_\infty}{(R/\text{inch})_n}$
$(R/\text{inch})_\infty$	free-stream Reynolds number per inch, $\frac{U_\infty}{\nu_\infty}$
T_∞	free-stream static temperature
T_o	total temperature
T_n	static temperature based on bluntness reduced Mach number (M_n), $\frac{T_o}{1 + 0.2 M_n^2}$
T_w	wall temperature
U_∞	free-stream velocity
U_n	velocity based on bluntness reduced Mach number (M_n), $(49 \sqrt{T_n}) M_n$

x_t	distance from leading edge to end of transition
Y_c	height above surface where maximum fluctuation energy is indicated as defined in reference 1 (see chart 4 herein)
$\frac{Y_c}{\delta_t}$	ratio of critical layer to boundary-layer thickness used in defining b_1 , essentially, $\frac{Y_c}{\delta_t} \cong \frac{\delta_t^*}{\delta_t}$ (see chart 4 and eqs. (A7) and (A8))
Y_n	thickness of bluntness reduced Mach number and unit Reynolds number layer (see sketches (b) and (c))
Y_{SB}	perpendicular distance to the horizontal plane of symmetry from the sonic point on the body (see sketches (b) and (c))
γ	ratio of specific heats (assumed to be 1.4 for air)
δ_t	boundary-layer thickness
δ_t^*	boundary-layer displacement thickness
Λ	leading-edge sweep
μ_∞	viscosity based on T_∞
μ_n	viscosity based on T_n
ν_n	kinematic viscosity based on T_n

CHARTS FOR ESTIMATING BOUNDARY-LAYER TRANSITION
ON FLAT PLATES

Edward J. Hopkins, Don W. Jillie, and Virginia L. Sorensen

Ames Research Center

SUMMARY

Charts are presented for rapidly estimating the end of boundary-layer transition for flat-plate wind-tunnel models with supersonic leading edges at an angle of attack of 0° . The charts were developed from the semiempirical method of Deem and Murphy who derived an equation that accounts for the combined effects of Mach number, unit Reynolds number, leading-edge sweep, leading-edge bluntness, and wall temperature on transition Reynolds number.

INTRODUCTION

For wind-tunnel tests, it is necessary to know the condition of the boundary layer so that the results can be interpreted correctly for extrapolation to flight Reynolds numbers. In addition, at hypersonic Mach numbers it is important to know whether the boundary layer is laminar or turbulent both from the standpoint of drag and of heat transfer.

Until recently no integrated method existed for estimating the end of boundary-layer transition since so many factors were known to affect transition; therefore, emphasis in past investigations was placed on a separate evaluation of each factor. Many of these factors are discussed in references 2 and 3. Deem and Murphy developed a semiempirical equation in reference 2 by which five important variables known to affect transition can be taken into account: Mach number, unit Reynolds number, leading-edge sweep, leading-edge bluntness, and wall temperature. The method was developed from data on "aerodynamically" smooth models having surface roughness less than that required to influence boundary-layer transition. Since the data were taken in wind tunnels with different turbulence levels, the results should be considered as only representative average transition Reynolds numbers. The method is, furthermore, only applicable to flat-plate models with supersonic leading edges at an angle of attack of 0° . Examination of 291 experimental points in reference 2 gave a standard deviation of 33 percent between the measured and calculated transition Reynolds numbers. However, much of this deviation can be explained on the basis of variations in wind-tunnel turbulence and imprecise measurements of transition and leading-edge bluntness.

The charts presented are based on the semiempirical method of reference 2 and offer a simple method for determining the approximate end of transition for flat plates mounted in wind tunnels. The charts cover ranges of

leading-edge sweep from 0° to 80° , unit Reynolds numbers from 10^3 to 10^7 per inch, Mach numbers from 1.1 to 12, and leading-edge thicknesses from 0 to 0.5 inch.

Although the charts presented are based on wind-tunnel transition results, they should be useful in making a first approximation of the minimum amount of laminar flow to be expected in flight. In general, transition Reynolds numbers in flight are expected to be higher than in wind tunnels, as evidenced by figure 3 of reference 4. By firing a hollow cylinder into still air, James (ref. 5) obtained nearly four times the transition Reynolds number as did the present authors for a flat plate mounted in a wind tunnel, although both models had nearly the same leading-edge thickness. Moreover, transition Reynolds numbers as high as 33 million were measured at a Mach number of 3.15 when large highly stabilized cone-cylinder rockets were fired into the atmosphere (ref. 6).

DESCRIPTION OF THE DEEM AND MURPHY METHOD

The important concepts and assumptions involved in the Deem and Murphy method for predicting transition Reynolds number will be described briefly. Some sketches will be included to help in the interpretation of certain bluntness criteria. The method is restricted to flat-plate wind-tunnel models having aerodynamically smooth surfaces. In addition, the method as developed is only applicable to models at an angle of attack of 0° with supersonic leading edges of nearly semicircular cross section. The method should be applicable, however, to models at small angles of attack provided the local flow conditions above the model are used in the equations. (If the leading edge is subsonic, the transition process is more complex because of the formation of a leading-edge "bubble," see ref. 4.) The method accounts for the effects of five quantities known to effect transition: Mach number, leading-edge bluntness, leading-edge sweep, wall temperature, and unit Reynolds number.

Mach Number

Whitfield and Potter (ref. 7) showed that transition Reynolds number for zero leading-edge bluntness ($R_{t,0}$) increased over five times when the Mach number was increased from about 3 to 8. This increase in $R_{t,0}$ cannot be explained on the basis of the physical leading-edge bluntness reducing the unit Reynolds number (Moeckel effect, ref. 8), since the values of $R_{t,0}$ were obtained by extrapolation of data curves to zero bluntness. Deem and Murphy (ref. 2) empirically derived an equation from existing data, after reducing the data to a common unit Reynolds number of 3×10^5 per inch, to give this Mach number effect as

$$R_{t,0} = 1 \times 10^6 + 0.36 \times 10^6 |M_\infty - 3|^{3/2} \quad (1)$$

Whitfield and Potter found that R_t did not reach a limit even though some of their data for models with blunt leading edges were obtained close to

the bluntness Reynolds number (R_b) required according to Moeckel's analysis for maximum influence (i.e., $R_b \approx 3000$). To account for this insufficiency of the Moeckel effect alone giving the correct prediction of R_t , Whitfield and Potter empirically derived the following approximate formula for transition Reynolds number

$$R_{t,1} = (R_{t,o} \text{ for } M_\infty) \frac{(R/\text{inch})_\infty}{(R/\text{inch})_n} \left(\frac{R_{t,o} \text{ for } M_n}{R_{t,o} \text{ for } M_\infty} \right) \quad (2)$$

Deem and Murphy's equation (1) written in terms of the bluntness reduced Mach number becomes

$$(R_{t,o} \text{ for } M_n) = (R_{t,o})_n = 1 \times 10^6 + 0.36 \times 10^6 |M_n - 3|^{3/2} \quad (3)$$

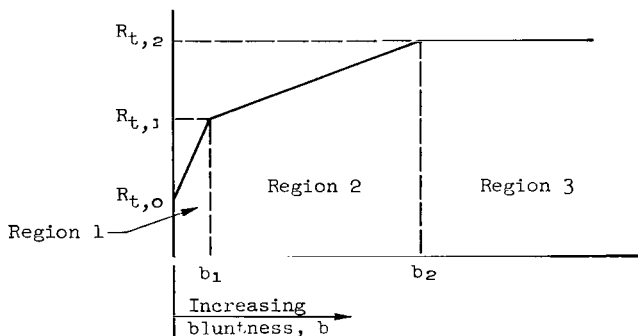
In the Deem and Murphy method, it is assumed that equation (2) applies for relatively sharp leading edges, but that for very blunt leading edges only the reduced unit Reynolds number (Moeckel effect) applies; therefore, the equation for R_t becomes

$$R_{t,2} = (R_{t,o} \text{ for } M_\infty) \frac{(R/\text{inch})_\infty}{(R/\text{inch})_n} \quad (4)$$

in which $(R_{t,o} \text{ for } M_\infty) = R_{t,o}$ from equation (1). In the next section the leading-edge bluntness criteria for using equation (2) or (4) will be discussed.

Leading-Edge Bluntness

A typical curve representing the variation of R_t with bluntness for an unswept plate having a semicircular leading edge was derived by Deem and Murphy from a limited amount of data and is shown in sketch (a). Deem and



Sketch (a)

Murphy assumed that $R_{t,1}$ was predictable by the Whitfield-Potter equation (2) and that $R_{t,2}$ was predictable by the Moeckel equation (4). The value of $R_{t,o}$ is determined by the empirical equation (1). To find the transition Reynolds number within regions 1 and 2 of sketch (a) it was assumed that a linear interpolation could be made as shown. It follows that the equation defining the transition Reynolds number for region 1 is

$$R_t = R_{t,o} + \frac{b}{b_1} (R_{t,1} - R_{t,o}) \quad (5)$$

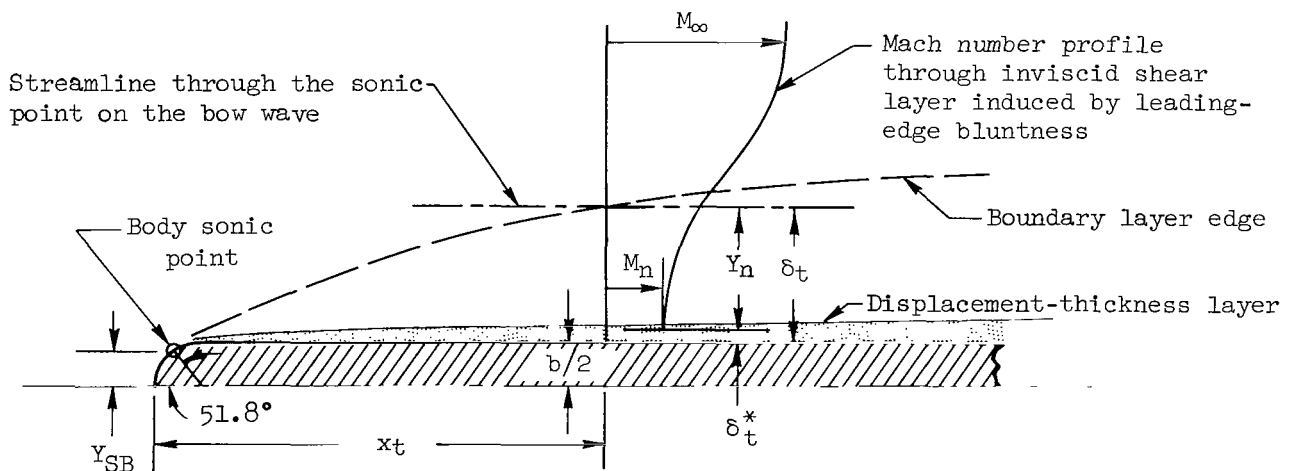
for region 2,

$$R_t = R_{t,1} + \frac{b - b_1}{b_2 - b_1} (R_{t,2} - R_{t,1}) \quad (6)$$

and for region 3,

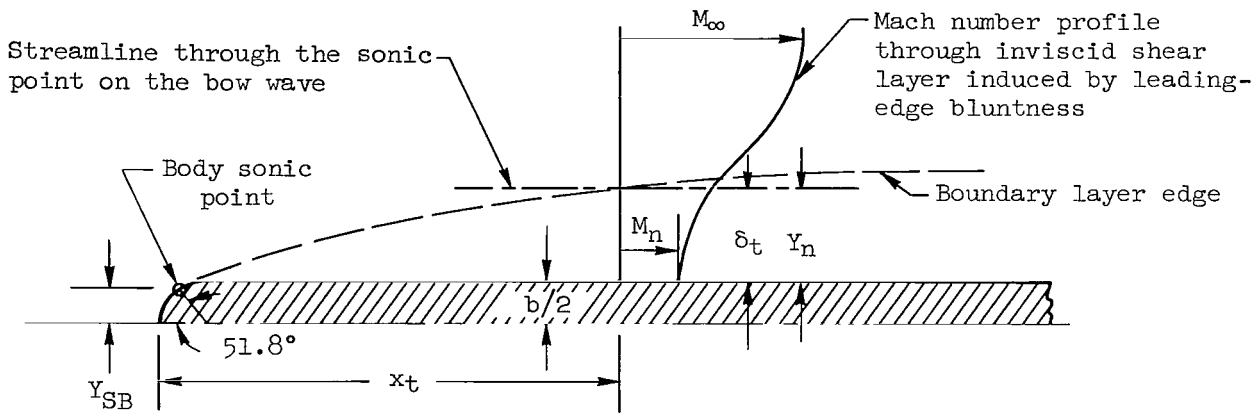
$$R_t = R_{t,o} \frac{(R/\text{inch})_\infty}{(R/\text{inch})_n} \quad (7)$$

In order to use equations (5) through (7) it is necessary to establish the bluntness criteria (b_1 and b_2) required to define the regions of sketch (a). Deem and Murphy accomplished this by analyzing a limited amount of experimental data. They found that good correlation is obtained for predicting transition Reynolds number provided b_1 and b_2 are defined in terms of the thickness of the bluntness reduced Mach number layer (Y_n) relative to the boundary-layer thickness. For b_1 , the displacement thickness was accounted for in defining the critical thickness of the reduced Mach number layer, but for b_2 the displacement thickness was ignored. Geometrical details¹ and equations defining b_1 and b_2 are presented with sketches (b) and (c), respectively.



Sketch (b).- Geometrical details for b_1 .

¹In either sketch (b) or (c), M_n is the bluntness reduced Mach number determined from the ratio of the total pressure behind the normal shock at the leading edge to the free-stream static pressure. After Moeckel, M_n is considered to be nearly the same as the Mach numbers within the shear-layer height (Y_n), and, therefore, is used in this manner to simplify the calculations.



Sketch (c).- Geometrical details for b_2 .

From sketch (b), following Moeckel's assumption regarding the critical bluntness for full bluntness effect on transition, for a flat-plate model with a semicircular leading edge²

$$Y_{SB} = \frac{b}{2} \sin 51.8^\circ \quad (8)$$

$$Y_n = \delta_t - \delta_t^* \quad (9)$$

Dividing equation (9) by (8) and solving for b , we obtain

$$b = \frac{2}{\sin 51.8^\circ} \left(\frac{\delta_t}{Y_n/Y_{SB}} \right) \left(1 - \frac{\delta_t^*}{\delta_t} \right) \quad (10)$$

Using experimental data and equation (10) for which bluntness was a variable and Y_n/Y_{SB} was considered a parameter, Deem and Murphy found that b_1 could be determined provided $Y_n/Y_{SB} = 3$, a value found to be independent of free-stream Mach number. Therefore, the equation for b_1 becomes

$$b_1 = \left(\frac{2.545}{3} \right) (\delta_t) \left(1 - \frac{\delta_t^*}{\delta_t} \right) \quad (11)$$

²The development in reference 2 is based on an assumed semicircular leading edge. Such a leading edge is generally representative of a so-called sharp leading edge and small departures from such a shape will not alter the results greatly.

This bluntness criterion differs from that of Moeckel (ref. 8) for which Y_n/Y_{SB} was shown to vary with free-stream Mach number. This difference is related, evidently, to Deem and Murphy's choice of iterating on equation (10) with experimental data and by obtaining best correlation by using two different bluntness criteria, b_1 and b_2 .

For models with very blunt leading edges relative to the transition-point boundary-layer thickness (region 3 of sketch (a)), the experimental transition data examined by Deem and Murphy indicated good correlation if the displacement thickness is ignored in the definition of b_2 . For this case, as shown in sketch (c), the reduced Mach number inviscid shear layer is measured from the model surface. The ratio Y_n/Y_{SB} was again considered to be a parameter but was found, from experimental data and equation (10), to have a value of 1.0, independent of Mach number. According to Deem and Murphy's empirical findings the equation for b_2 can be written from equation (10) (with $\delta_t^* \rightarrow 0$ and $Y_n/Y_{SB} = 1$) as

$$b_2 = \left(\frac{2}{\sin 51.8^\circ} \right) \left(\frac{\delta_t}{Y_n/Y_{SB}} \right) = 2.545 \delta_t \quad (12)$$

Leading-Edge Sweep

Leading-edge sweep can affect boundary-layer transition in two ways: First, when the leading edges are supersonic, the Moeckel effect (reduced unit Reynolds number due to leading-edge bluntness) becomes progressively smaller as sweep is increased because of the reduced strength of the leading-edge shock; that is, a constant assumed transition Reynolds number based on local flow contributions corresponds to a progressively smaller transition Reynolds number based on free-stream conditions as sweep increases, because the local unit Reynolds number also increases. The validity of the Moeckel assumption as applied to sweep was demonstrated in reference 4 in which it was shown that when the leading edge is supersonic, the transition Reynolds number decreases, at least qualitatively, with increases in sweep, as predicted, and that at a Mach number of 0.27 the transition Reynolds number remains nearly constant with increases in sweep to about 30° . Second, with both subsonic and supersonic leading edges, the variable crossflow within the boundary layer creates a twisted boundary-layer profile that can lead to boundary-layer instability and transition when a certain critical crossflow Reynolds number is reached, as suggested by Owen and Randall (ref. 9). Evidence that this phenomenon does occur is given in references 9 and 10.

Deem and Murphy semiempirically accounted for both the above sweep effects in the following manner:

1. In all three regions of sketch (a), $R_{t,o}$ or $(R_{t,o})_n$ is multiplied by the factor $\sqrt{\cos \Lambda}$. The reason this factor improved the correlation of the data is probably related to a decrease in effective bluntness as sweep increases.

2. In regions 2 and 3 at sweep angles greater than 25° , it is assumed that crossflow is dominant in affecting transition and that the total effect of sweep on transition can be approximated by multiplying $R_{t,0}$ by the $\sqrt{\cos \Lambda}$ factor without any further corrections for bluntness on either Mach number or unit Reynolds number.

3. In region 2 for sweep angles less than 25° and in region 1 for all sweep angles, both crossflow and bluntness are considered important; therefore, the $\sqrt{\cos \Lambda}$ factor is used with the bluntness reduced Mach number and unit Reynolds number factors.

4. In region 3 for sweep angles less than 25° , only the $\sqrt{\cos \Lambda}$ factor is used with the bluntness reduced unit Reynolds number.

Wall Temperature

The effect of wall temperature is accounted for in the method indirectly through the boundary-layer thickness equation used to define the bluntness criteria. Thus, by this treatment the transition Reynolds number is affected by wall temperature only in regions 1 and 2 and not at all in region 3 (with $b \gg b_2$).

Unit Reynolds Number

According to an analysis of existing data made by James (ref. 5), the variation of transition Reynolds number with unit Reynolds number can be expressed as

$$\log_{10} R_t = C_1 + 0.4 \log_{10} (R/\text{inch})_\infty \quad (13)$$

where C_1 is dependent on many variables. In the Deem and Murphy method C_1 is assumed to depend on the four variables: Mach number, leading-edge bluntness, leading-edge sweep, and temperature; and the second term in equation (13) is used to predict the effect of unit Reynolds number.

For completeness, the equations used for the calculations are summarized in appendix A. A more detailed development of the equations is given in reference 2.

PRESENTATION OF RESULTS

Chart 1 gives the effect of Mach number ($M = 1.1$ to 12) on transition Reynolds number for various leading-edge thicknesses ($b = 0.0001$ to 0.5 inch) and unit Reynolds numbers ($(R/\text{inch}) = 10^3$ to 10^7). Chart 2 gives the effect of Mach number ($M_\infty = 1.1$ to 12) on the normalized transition Reynolds number for various angles of sweep ($\Lambda = 0$ to 80°), unit Reynolds numbers

$((R/\text{inch})_\infty = 10^3 \text{ to } 10^7)$ and leading-edge thicknesses ($b = 0.0001 \text{ to } 0.5 \text{ inch.}$)^{3,4} In both sets of charts the wall temperature and the total temperature were held constant at 400° R and 500° R , respectively. A limited study of the effects of large temperature changes on the transition measured on flat plates indicated that temperature effects were small and were adequately accounted for by the slight indirect effect on boundary-layer thickness as contained in the method. This may seem contrary to the commonly accepted large variations in transition due to surface cooling; however, the latter effects may be related to the three dimensionality of the flow. Calculated transition results presented in chart 3 for two different Mach numbers and unit Reynolds numbers for the unswept case show a very small effect due to temperature changes. Since the method should be considered only for obtaining approximate values of transition Reynolds number, no additional corrections for this secondary effect of wall-temperature ratio appear justified.⁵

Sample Calculation

It will be assumed that the following conditions exist on a flat plate:

$$M_\infty = 6.0$$

$$(R/\text{inch})_\infty = 10^6$$

$$b = 0.01 \text{ inch}$$

$$\Lambda = 60^\circ$$

From chart 1(d), $(R_t)_{\Lambda=0} = 1.4 \times 10^7$ and from chart 2(d), $R_t/(R_t)_{\Lambda=0} = 0.23$ for the above conditions. The transition Reynolds number is

³Note that for a particular sweep angle the minimum Mach number shown is that at which the leading edge first becomes sonic. It is shown in reference 4 that when the leading edge becomes subsonic, transition moves close to the leading edge because of the influence of a localized leading-edge separation "bubble."

⁴The sharp discontinuities in some of the curves presented in charts 2(d) and 2(e) are related to the arbitrariness in defining the bluntness, b . In real flow, the curves would probably have a smoother variation with Mach number than shown.

⁵Chart 2 should be applicable to flight vehicles as well as wind-tunnel models. Chart 1, however, should be restricted to wind-tunnel models or used to estimate the minimum expected transition Reynolds number for flight, because the transition Reynolds numbers given were derived from wind-tunnel experiments in which wall disturbances and free-stream turbulence were present. The usually large difference in static temperature for wind-tunnel and flight models, however, is not expected to have an important influence on transition, provided the surfaces are relatively flat.

$$R_t = (R_t)_{\Lambda=0} \left[R_t / (R_t)_{\Lambda=0} \right] = 3.2 \times 10^6$$

CONCLUDING REMARKS

From the charts presented, a rapid estimate can be made of the boundary-layer transition on flat-plate models mounted in wind tunnels. These charts are restricted to models with supersonic leading edges at an angle of attack of 0° . Mach number, unit Reynolds number, leading-edge bluntness, sweep, and wall temperature are the variables considered. The wall temperature was shown for flat plates to be of secondary importance in affecting transition; therefore, the charts are presented for a single wall temperature.

It should be emphasized that these charts give only an approximate transition Reynolds number for flat plates mounted in wind tunnels. Since in flight the maximum obtainable transition Reynolds numbers should be considerably higher than those for a wind tunnel, the charts should be used only to obtain a first approximation of the minimum transition Reynolds number expected for flight vehicles.

Ames Research Center
National Aeronautics and Space Administration
Moffett Field, Calif., 94035, April 2, 1970

APPENDIX A

EQUATIONS USED FOR CALCULATING TRANSITION REYNOLDS

NUMBER BY THE DEEM AND MURPHY METHOD

BASIC TRANSITION REYNOLDS NUMBER EQUATION

The basic equation for calculating transition Reynolds number is

$$\log_{10} R_t = C_1 + 0.4 \log_{10} (R/\text{inch})_{\infty} \quad (\text{A1})$$

where C_1 depends on Mach number, leading-edge bluntness, leading-edge sweep, and wall temperature. The second term in equation (A1) is considered independent of C_1 and accounts for the unit Reynolds number effect.

REDUCED MACH NUMBER AND UNIT REYNOLDS NUMBER EQUATIONS

In the method, transition Reynolds number is affected by changes in Mach number and unit Reynolds number near the surface resulting from leading-edge bluntness and the associated leading-edge shock losses. In reference 4, expressions were given for these reduced numbers for which $\gamma = 1.4$ was assumed.¹ The same expressions are given below:

$$M_n = \left(5 \left\{ \left(\frac{6}{7M_{\infty}^2 \cos^2 \Lambda - 1} \right)^{5/2} \left[\frac{6M_{\infty}^2 \cos^2 \Lambda (M_{\infty}^2 + 5)}{5(M_{\infty}^2 \cos^2 \Lambda + 5)} \right]^{7/2} \right\}^{2/7} - 5 \right)^{1/2} \quad (\text{A2})$$

and

$$\frac{(R/\text{inch})_n}{(R/\text{inch})_{\infty}} = \frac{M_n}{M_{\infty}} \left(\frac{T_{\infty}}{T_n} \right)^{1/2} \frac{\mu_{\infty}}{\mu_n} \quad (\text{A3})$$

where

$$\frac{\mu_{\infty}}{\mu_n} = \frac{0.03665 T_{\infty} (T_n + 198.6)}{(T_n)^{3/2}} \quad \text{for } T_{\infty} < 200^{\circ} \text{ R and } T_n > 200^{\circ} \text{ R} \quad (\text{A4})$$

¹No explicit expressions for reduced Mach number or unit Reynolds number can be written when real gas effects are taken into account. Since the method of reference 2 is highly approximate and the real gas effects are known to be small, ignoring these effects seems justified.

or

$$\frac{\mu_{\infty}}{\mu_n} = \left(\frac{T_n + 198.6}{T_{\infty} + 198.6} \right) \left(\frac{T_{\infty}}{T_n} \right)^{3/2} \quad \text{for } T_{\infty} \text{ and } T_n > 200^{\circ} \text{ R} \quad (\text{A5})$$

and

$$T_n = \frac{T_o}{1 + 0.2M_n^2} \quad (\text{A6})$$

BLUNTNES CRITERIA, b_1 AND b_2

It is necessary to establish the value of the leading-edge bluntness, b , relative to the bluntness criteria, b_1 and b_2 , defined by equations (11) and (12). If Creager's equation is used for boundary-layer thickness as given in reference 11 and $Y_n/Y_{SB} = 3.0$ (as determined in ref. 2), equation (11) for small bluntness becomes

$$b_1 = \frac{2.545}{3} \left(1 - \frac{Y_c}{\delta_t} \right) \left(\frac{1.73T_w}{M_{\infty}^2 T_{\infty}} + 0.1328 + \frac{4.27}{M_{\infty}^2} \right) M_{\infty}^2 \\ \times \sqrt{\left(\frac{T_w}{T_{\infty}} \right)^{1/2} \left(\frac{T_{\infty} + 198.6}{T_w + 198.6} \right) \left[\frac{\sqrt{R_t}}{(R/\text{inch})_{\infty}} \right]} \quad \text{for } T_{\infty} \text{ and } T_w > 200^{\circ} \text{ R} \quad (\text{A7})^2$$

or

$$b_1 = \frac{2.545}{3} \left(1 - \frac{Y_c}{\delta_t} \right) \left(\frac{1.73T_w}{M_{\infty}^2 T_{\infty}} + 0.1328 + \frac{4.27}{M_{\infty}^2} \right) M_{\infty}^2 \\ \times \sqrt{\left(\frac{T_{\infty}}{T_w} \right) \frac{(T_w)^{3/2}}{0.03665 T_{\infty} (T_w + 198.6)} \left[\frac{\sqrt{R_t}}{(R/\text{inch})_{\infty}} \right]} \\ \text{for } T_w > 200^{\circ} \text{ R and } T_{\infty} \leq 200^{\circ} \text{ R} \quad (\text{A8})^{2,3}$$

²Since the unknown transition Reynolds number, R_t occurs in equations (A7), (A8), (A10), and (A11), it is necessary to obtain R_t by iteration with equation (A1) which contains C_1 . In turn, the proper equation for C_1 , given hereinafter, can only be determined after b_1 and b_2 have been calculated.

³In equations (A8) and (A11) the linear approximation to Keyes' viscosity equation (ref. 12) was used for temperatures equal to or below 200° R ; whereas Sutherland's viscosity formula (ref. 13) was used for temperatures above 200° R .

where Y_c/δ_t , as noted by Potter and Whitfield (ref. 1), is, essentially,

$$\frac{Y_c}{\delta_t} \cong \frac{\delta_t^*}{\delta_t} \quad (A9)$$

Values of Y_c/δ_t from reference 1 are presented in chart 4. If Creager's equation is modified for boundary-layer thickness to include the effect of bluntness on the local surface conditions ($M_\infty \rightarrow M_n$, $T_\infty \rightarrow T_n$, and $(R/\text{inch})_\infty \rightarrow (R/\text{inch})_n$) and if $Y_n/Y_{SB} = 1.0$ (as determined in ref. 2) is used, equation (12) for large bluntness⁴ becomes

$$b_2 = 2.545 \left(\frac{1.73T_w}{M_n^2 T_n} + 0.1328 + \frac{4.27}{M_n^2} \right) (M_n^2) \sqrt{\left(\frac{T_w}{T_n} \right)^{1/2} \frac{T_n + 198.6}{T_w + 198.6}}$$

$$\times \frac{\sqrt{R_t \left[\frac{(R/\text{inch})_n}{(R/\text{inch})_\infty} \right]}}{(R/\text{inch})_\infty \left[\frac{(R/\text{inch})_n}{(R/\text{inch})_\infty} \right]} \quad \text{for } T_n \text{ and } T_w > 200^\circ \text{ R} \quad (A10)^2$$

or

$$b_2 = 2.545 \left(\frac{1.73T_w}{M_n^2 T_n} + 0.1328 + \frac{4.27}{M_n^2} \right) (M_n^2) \sqrt{\left(\frac{T_n}{T_w} \right) \frac{(T_w)^{3/2}}{0.03665T_n(T_w + 198.6)}}$$

$$\times \frac{\sqrt{R_t \left[\frac{(R/\text{inch})_n}{(R/\text{inch})_\infty} \right]}}{(R/\text{inch})_\infty \left[\frac{(R/\text{inch})_n}{(R/\text{inch})_\infty} \right]} \quad \text{for } T_w > 200^\circ \text{ R and } T_n \leq 200^\circ \text{ R} \quad (A11)^{2,3}$$

TERM C_1 FOR EQUATION (A1)

Since the transition Reynolds number given by equation (A1) is dependent on C_1 which depends on sweep and the bluntness criterion (b relative to b_1 and b_2) which also contains R_T , it is necessary to use an iterative process to calculate R_T . The following equation defines C_1 and the required sweep and bluntness criterion:

²See footnote, p. 11.

³See footnote, p. 11.

⁴For this case, the entire boundary layer is engulfed in the Mach number reduced inviscid shear layer in which the Mach number is nearly constant and equal to M_n .

For $0 \leq b \leq b_1$, all sweep angles

$$C_1 = \log_{10} \left\{ (1 \times 10^6 + 0.36 \times 10^6 |M_\infty - 3|^{3/2}) (\cos \Lambda)^{1/2} \right. \\ \left. \times \left[1 + \frac{(R/\text{inch})_\infty}{(R/\text{inch})_n} \left(\frac{b}{b_1} \right) \left(\frac{1 \times 10^6 + 0.36 \times 10^6 |M_n - 3|^{3/2}}{1 \times 10^6 + 0.36 \times 10^6 |M_\infty - 3|^{3/2}} \right) - \frac{b}{b_1} \right] \right\} - 2.19 \quad (\text{A12})$$

For $b_1 \leq b \leq b_2$, $0 \leq \Lambda \leq 25^\circ$

$$C_1 = \log_{10} \left\{ (1 \times 10^6 + 0.36 \times 10^6 |M_n - 3|^{3/2}) (\cos \Lambda)^{1/2} \right. \\ \left. \times \frac{(R/\text{inch})_\infty}{(R/\text{inch})_n} \left[1 + \left(\frac{b - b_1}{b_2 - b_1} \right) \left(\frac{1 \times 10^6 + 0.36 \times 10^6 |M_\infty - 3|^{3/2}}{1 \times 10^6 + 0.36 \times 10^6 |M_n - 3|^{3/2}} \right) - \left(\frac{b - b_1}{b_2 - b_1} \right) \right] \right\} - 2.19 \quad (\text{A13})$$

For $b > b_2$, $0 \leq \Lambda \leq 25^\circ$

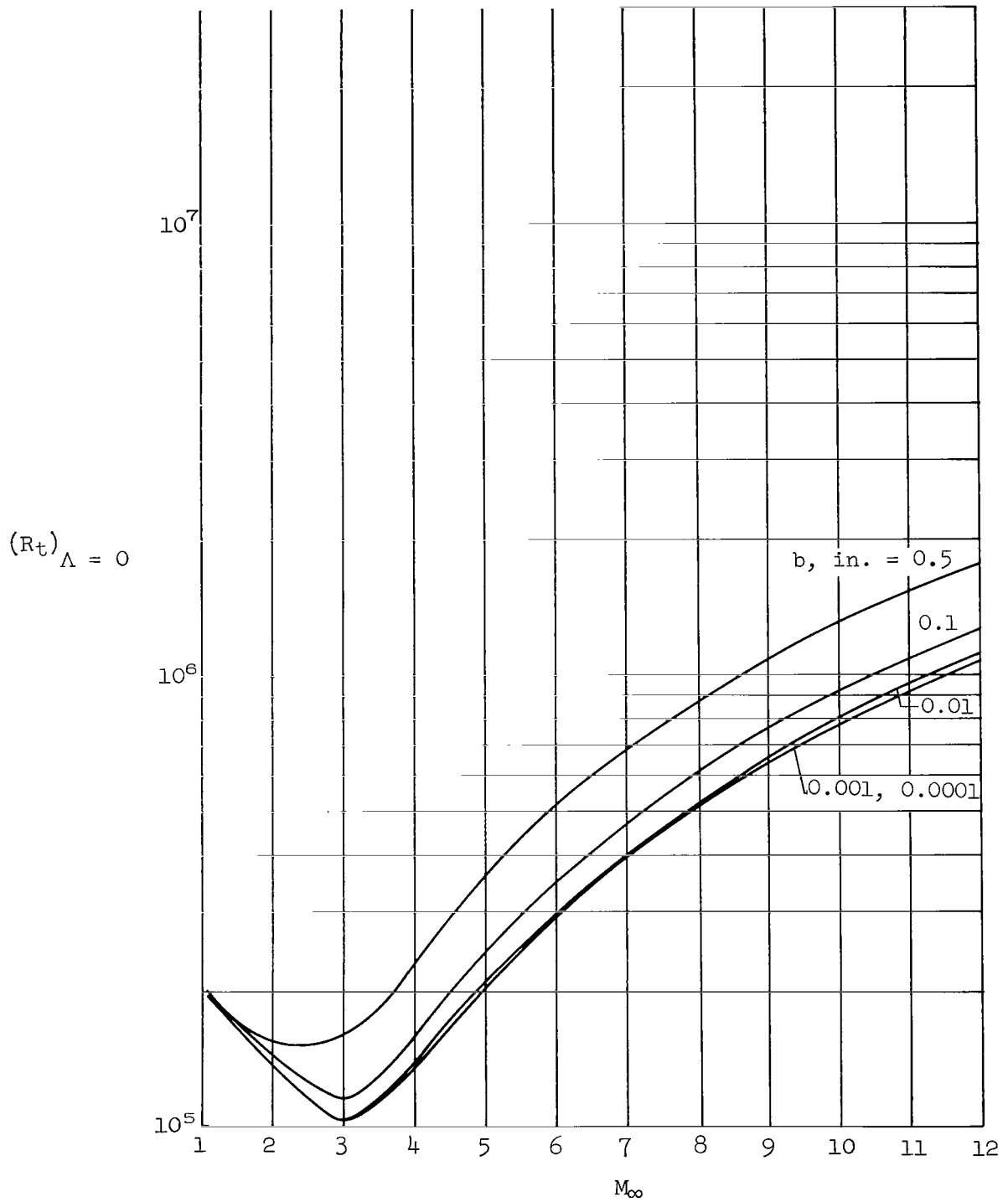
$$C_1 = \log_{10} \left\{ (1 \times 10^6 + 0.36 \times 10^6 |M_\infty - 3|^{3/2}) (\cos \Lambda)^{1/2} \left[\frac{(R/\text{inch})_\infty}{(R/\text{inch})_n} \right] \right\} - 2.19 \quad (\text{A14})$$

For $b > b_1$, $\Lambda > 25^\circ$

$$C_1 = \log_{10} \left[(1 \times 10^6 + 0.36 \times 10^6 |M_\infty - 3|^{3/2}) (\cos \Lambda)^{1/2} \right] - 2.19 \quad (\text{A15})$$

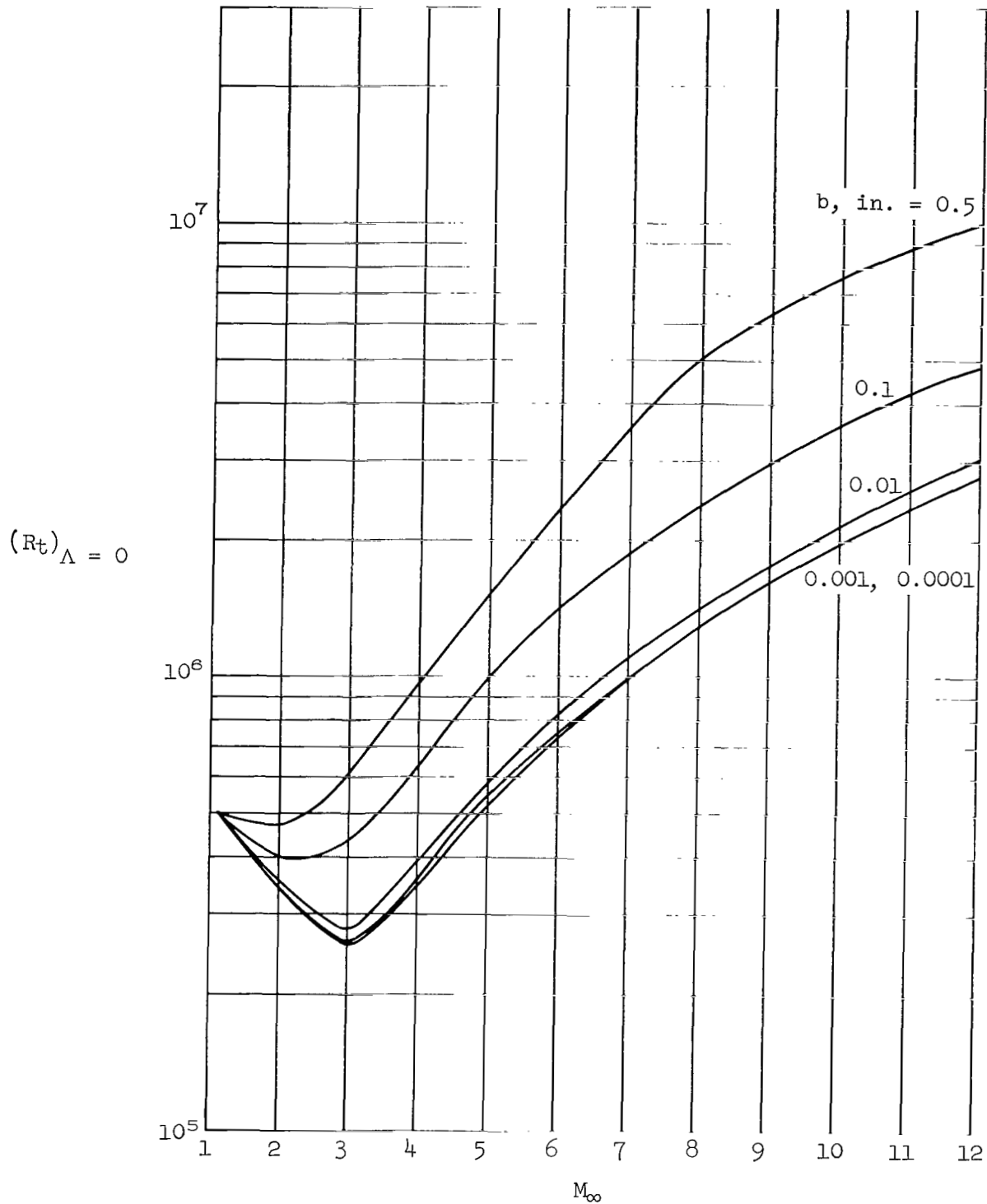
REFERENCES

1. Potter, J. L.; and Whitfield, J. D.: Effects of Slight Nose Bluntness and Roughness on Boundary-Layer Transition in Supersonic Flows. *J. Fluid Mech.*, vol. 12, Pt. 4, 1962.
2. Deem, R. E.; and Murphy, J. S.: Flat Plate Boundary Layer Transition at Hypersonic Speeds. AIAA Paper 65-128, 1965.
3. Markovin, Mark V.: Critical Evaluation of Transition From Laminar to Turbulent Flow. Proj. AF-1366, March 1969.
4. Jillie, Don W.; and Hopkins, Edward J.: Effects of Mach Number, Leading-Edge Bluntness, and Sweep on Boundary-Layer Transition on a Flat Plate. NASA TN D-1071, 1961.
5. James, Carlton S.: Boundary-Layer Transition on Hollow Cylinders in Supersonic Free Flight as Affected by Mach Number and a Screw-Thread Type of Surface Roughness. NASA MEMO 1-20-59A, 1959.
6. Merlet, Charles F.; and Rumsey, Charles B.: Supersonic Free-Flight Measurement of Heat Transfer and Transition of a 10° Cone Having a Low Temperature Ratio. NACA RM L56L10, 1957.
7. Whitfield, J. P.; and Potter, J. L.: The Influence of Slight Leading Edge Bluntness on Boundary-Layer Transition at a Mach Number of Eight. AEDC-TDR-64-18, 1964.
8. Moeckel, W. E.: Some Effects of Bluntness on Boundary-Layer Transition and Heat Transfer at Supersonic Speeds. NACA Rep. 1312, 1957.
9. Owen, P. R.; and Randall, D. G.: Boundary-Layer Transition on a Swept-Back Wing. RAE TM Aero. 277, May 1952.
10. Chapman, G. T.: Some Effects of Leading-Edge Sweep on Boundary Layer Transition at Supersonic Speeds. NASA TN D-1075, 1961.
11. Creager, M. O.: The Effect of Leading Edge Sweep and Surface Inclination on the Hypersonic Flow Field Over a Blunt Flat Plate. NASA MEMO 12-26-58A, 1959.
12. Bertram, Mitchel H.: Comment on "Viscosity of Air." *J. Spacecraft*, vol. 4, no. 2, Feb. 1967.
13. Ames Research Staff: Equation, Tables, and Charts for Compressible Flow. NACA Rep. 1135, 1953. (Supersedes NACA TN 1428.)



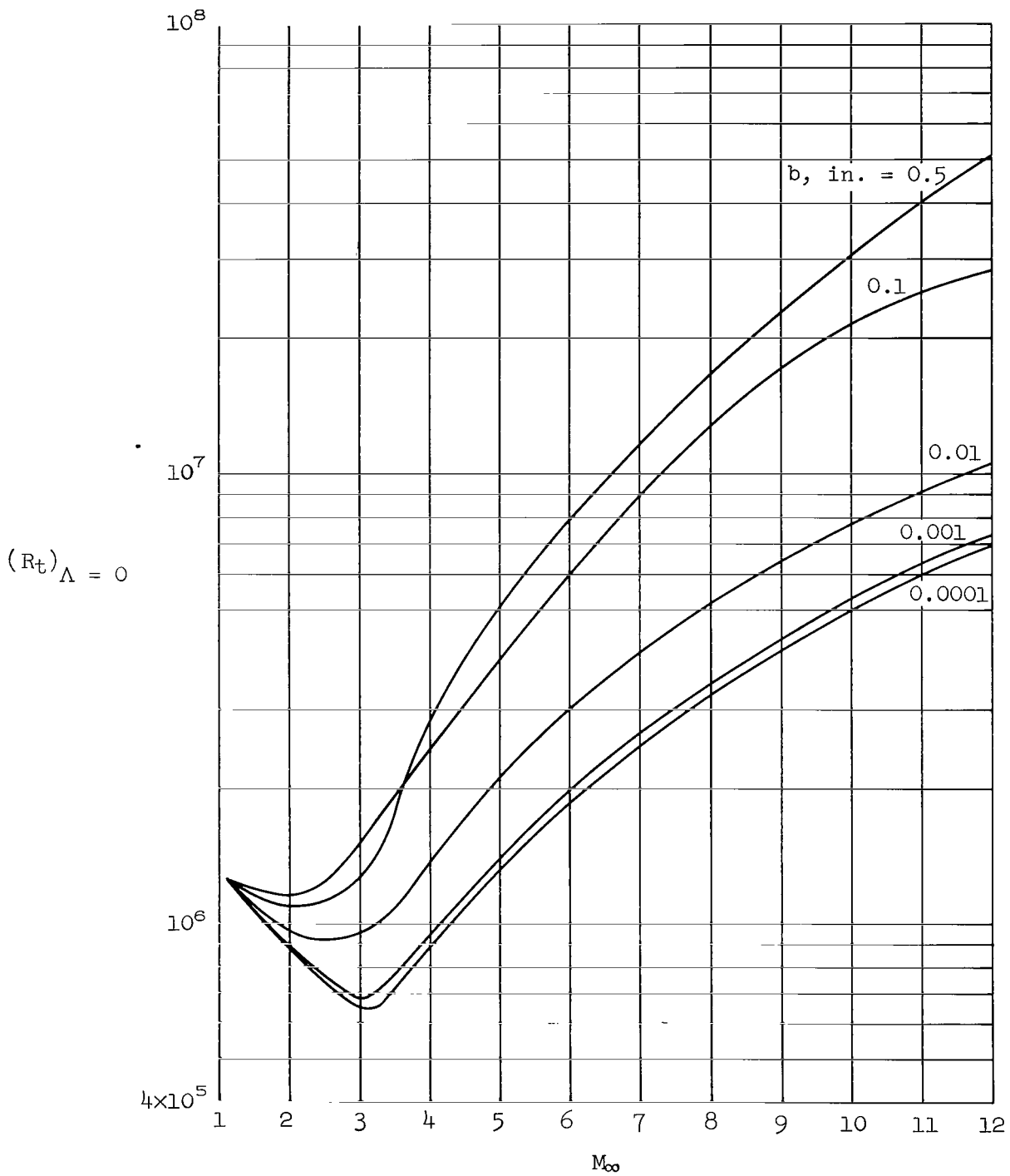
(a) $(R/\text{inch})_{\infty} = 10^3$

Chart 1.- Estimated effect of Mach number on transition Reynolds number for a flat plate with no leading-edge sweep; $T_w = 400^{\circ} \text{ R}$, $T_o = 500^{\circ} \text{ R}$.



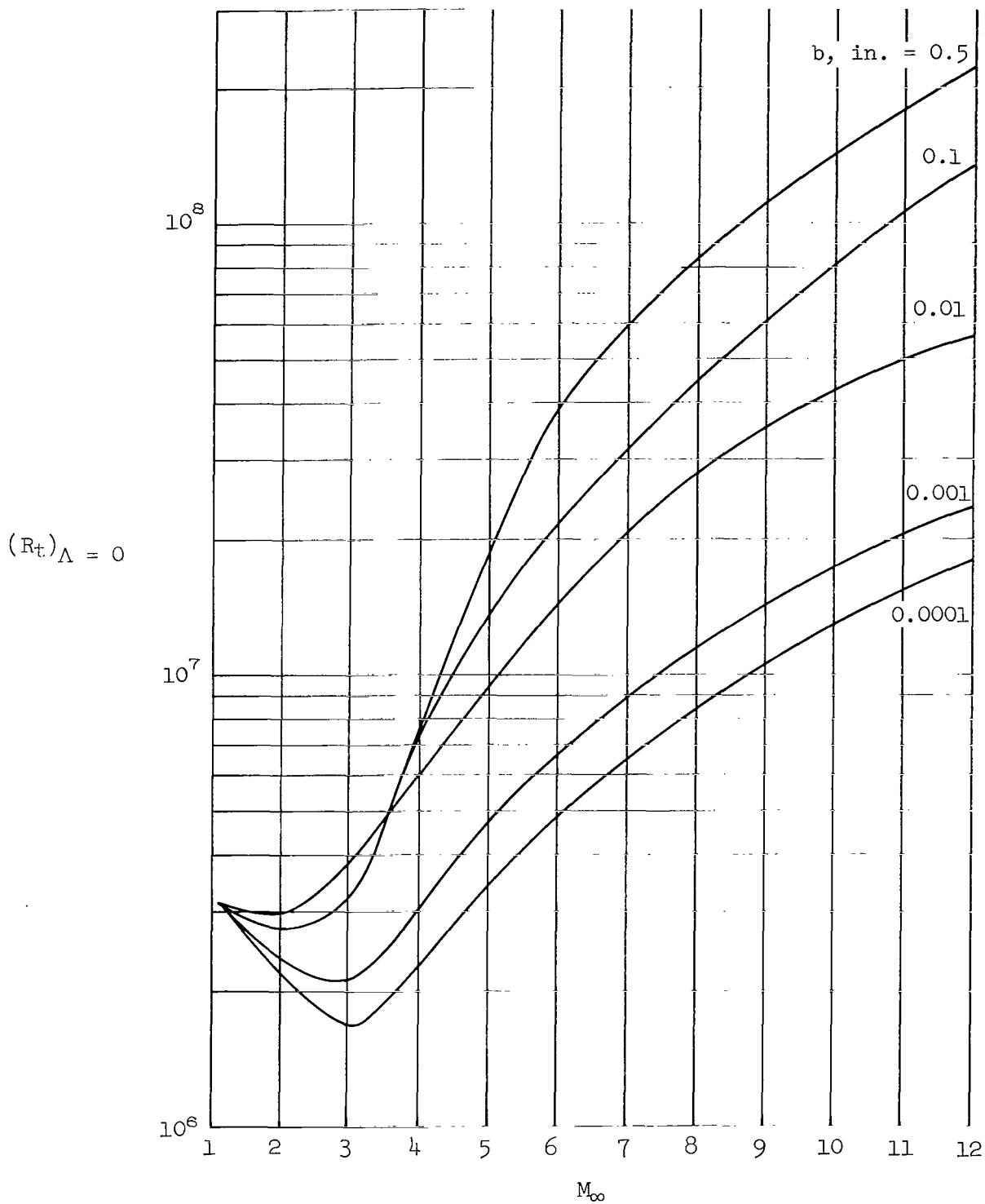
(b) $(R/\text{inch})_{\infty} = 10^4$

Chart 1.- Continued.



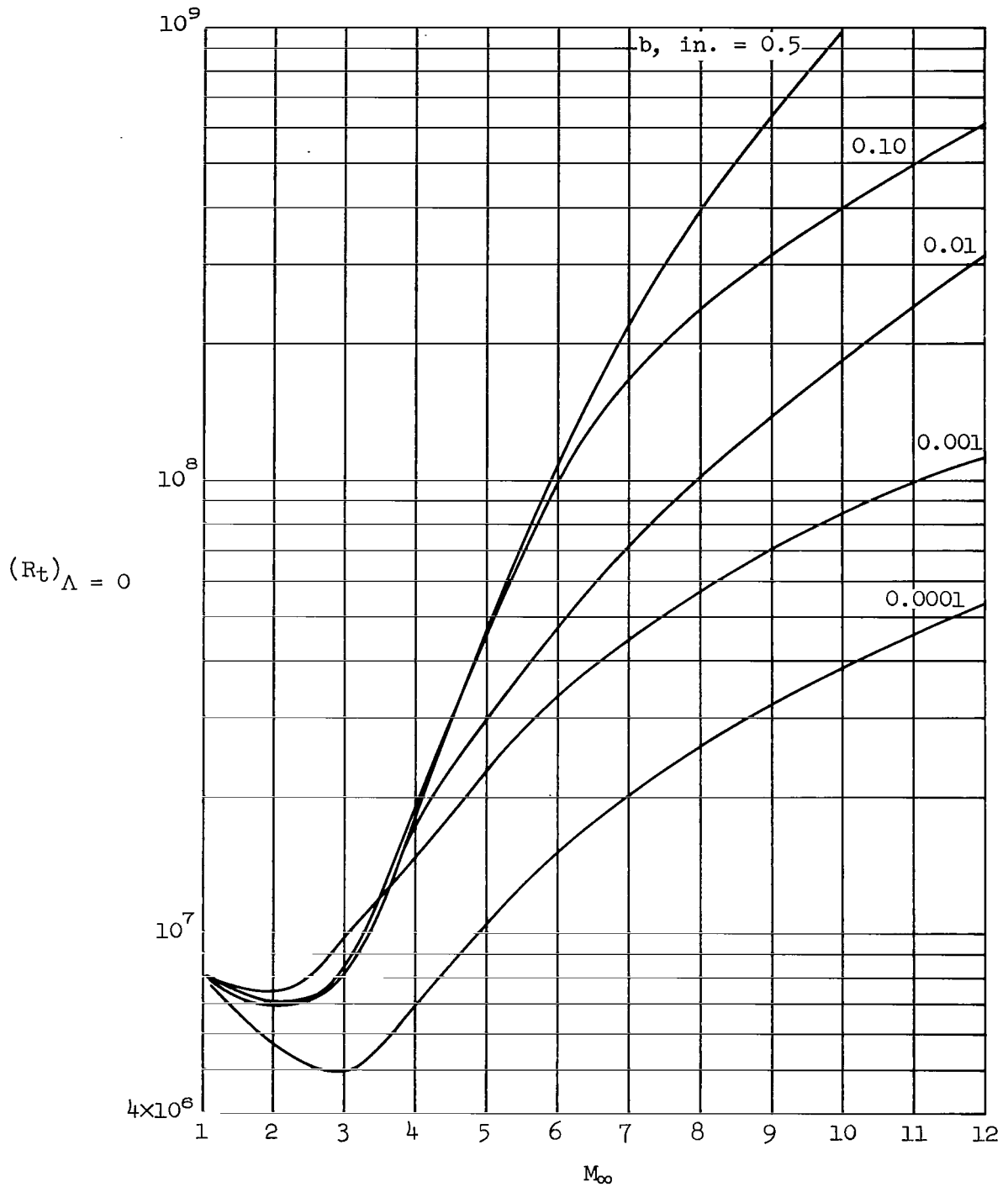
(c) $(R/\text{inch})_{\infty} = 10^5$

Chart 1.- Continued.



(d) $(R/\text{inch})_{\infty} = 10^6$

Chart 1.- Continued.



(e) $(R/\text{inch})_{\infty} = 10^7$

Chart 1.- Concluded.

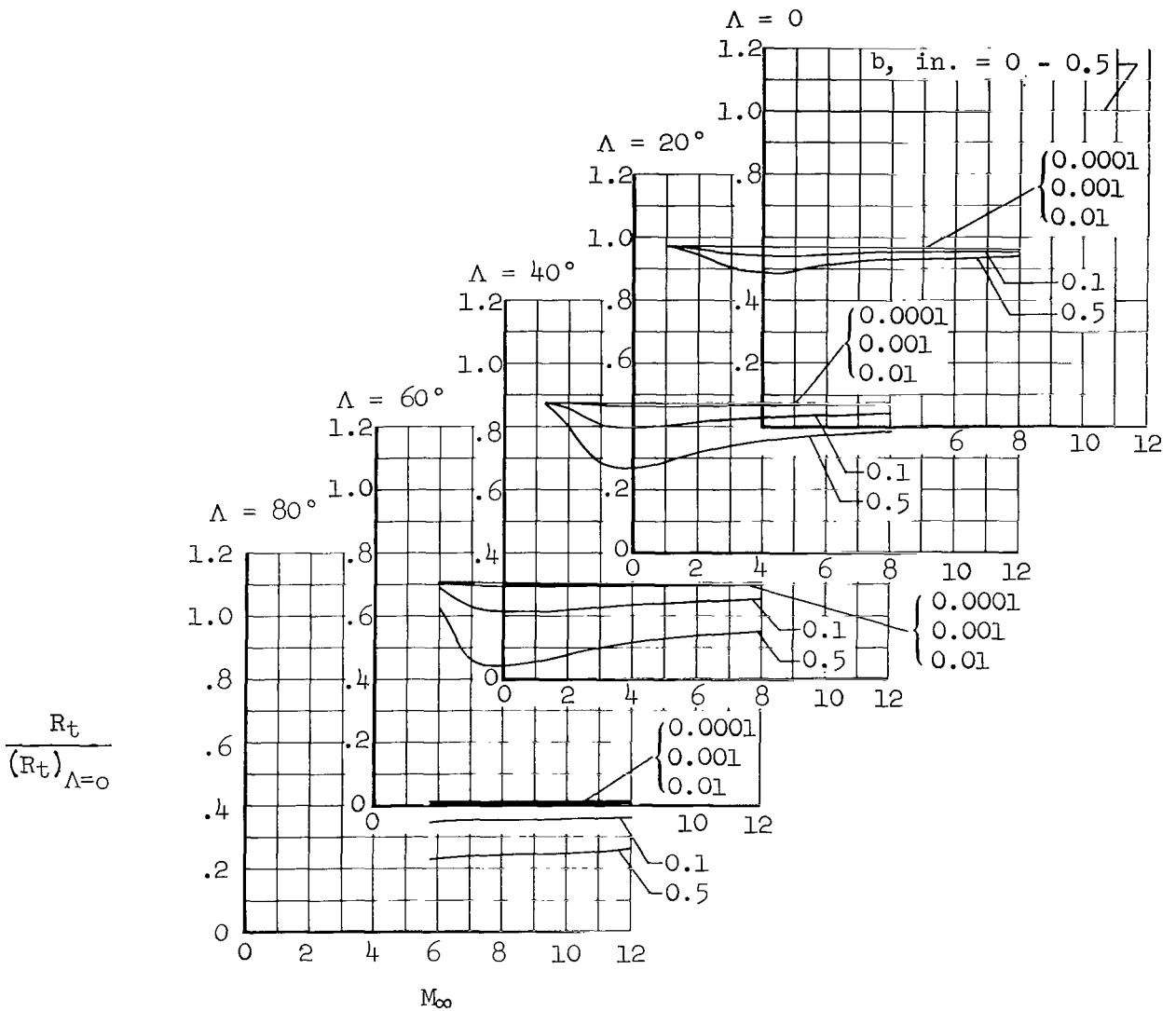


Chart 2.- Estimated effect of Mach number on normalized transition Reynolds number for a flat plate with various angles of leading-edge sweep; $T_w = 400^{\circ} R$, $T_o = 500^{\circ} R$.

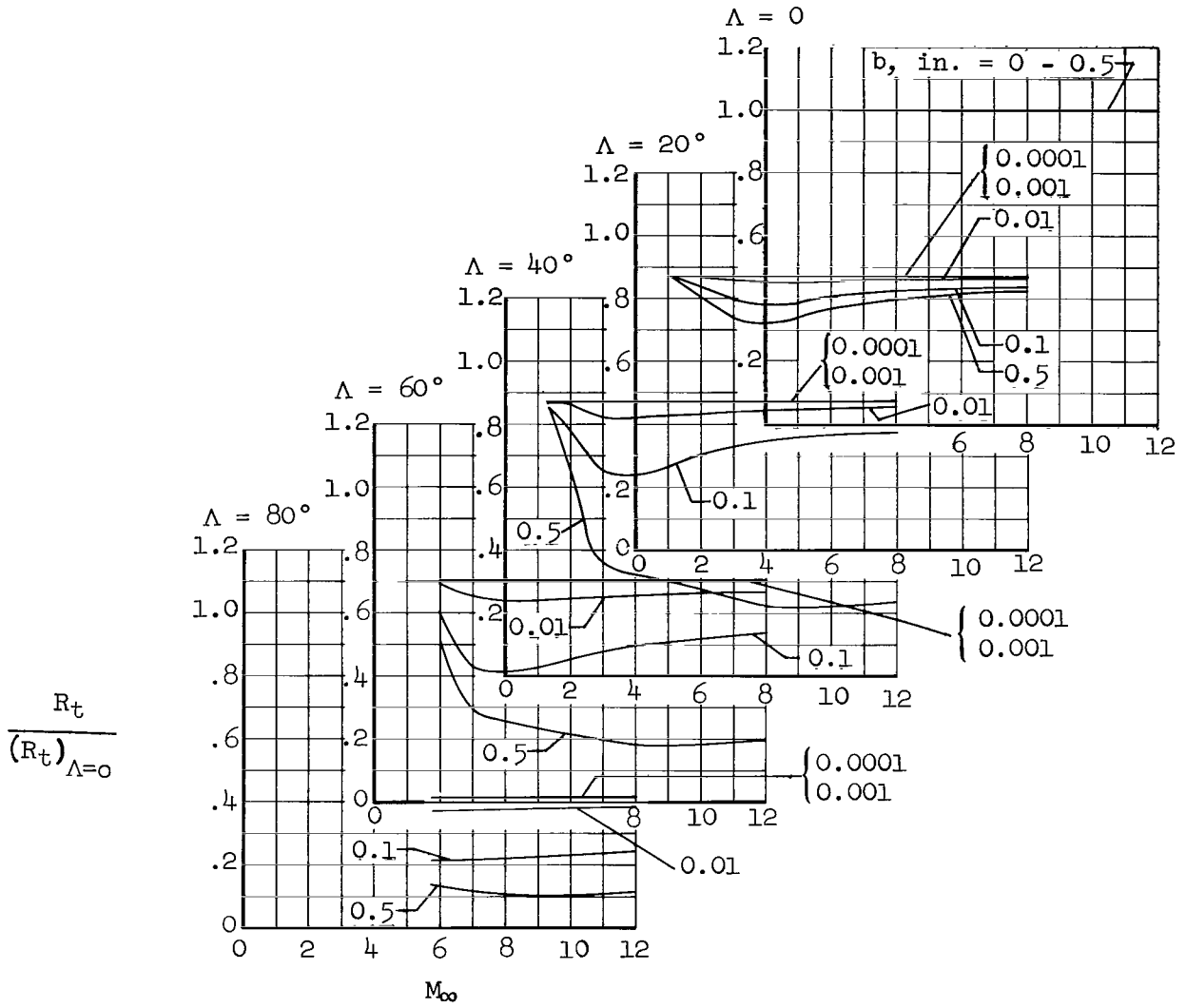
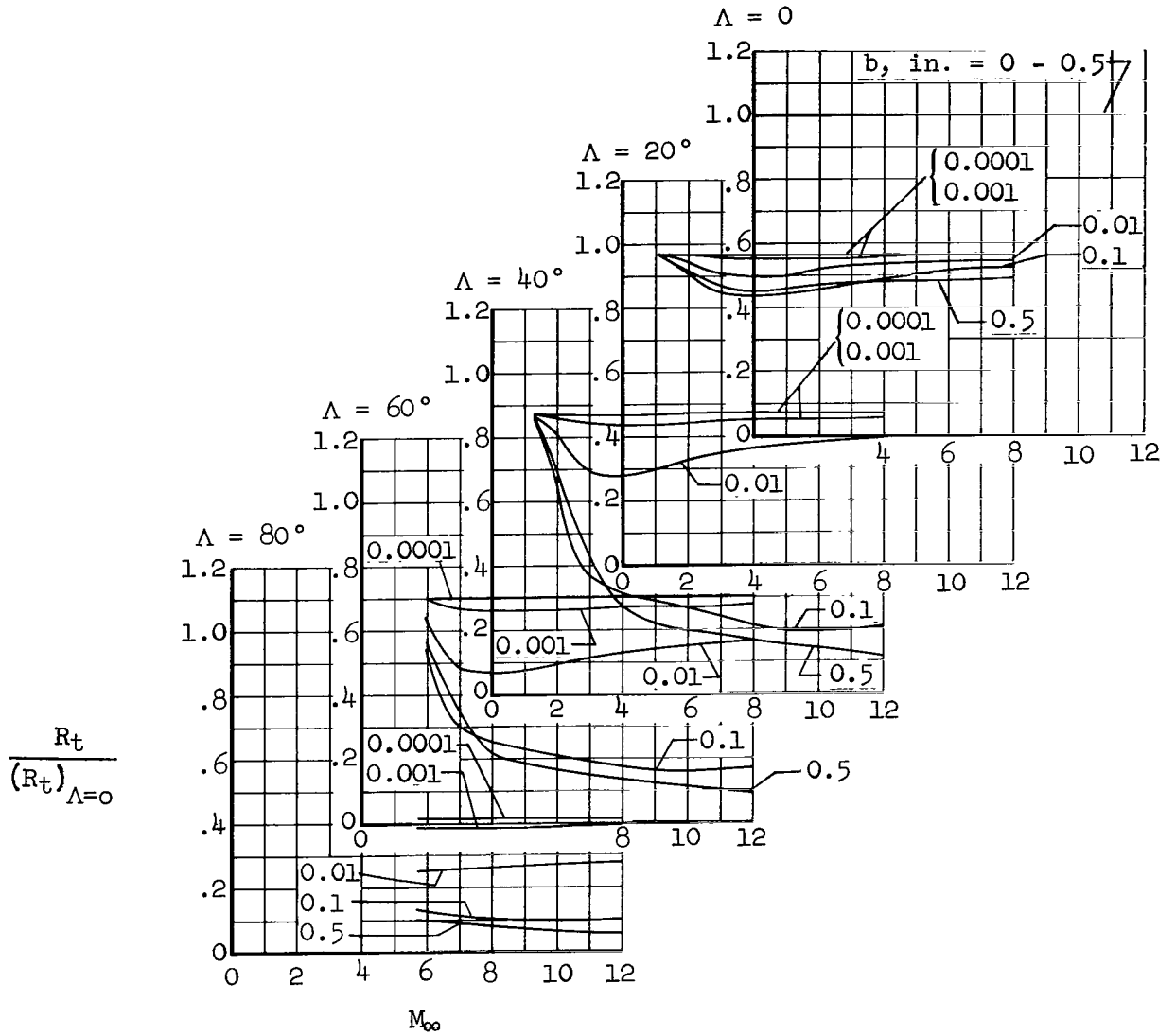
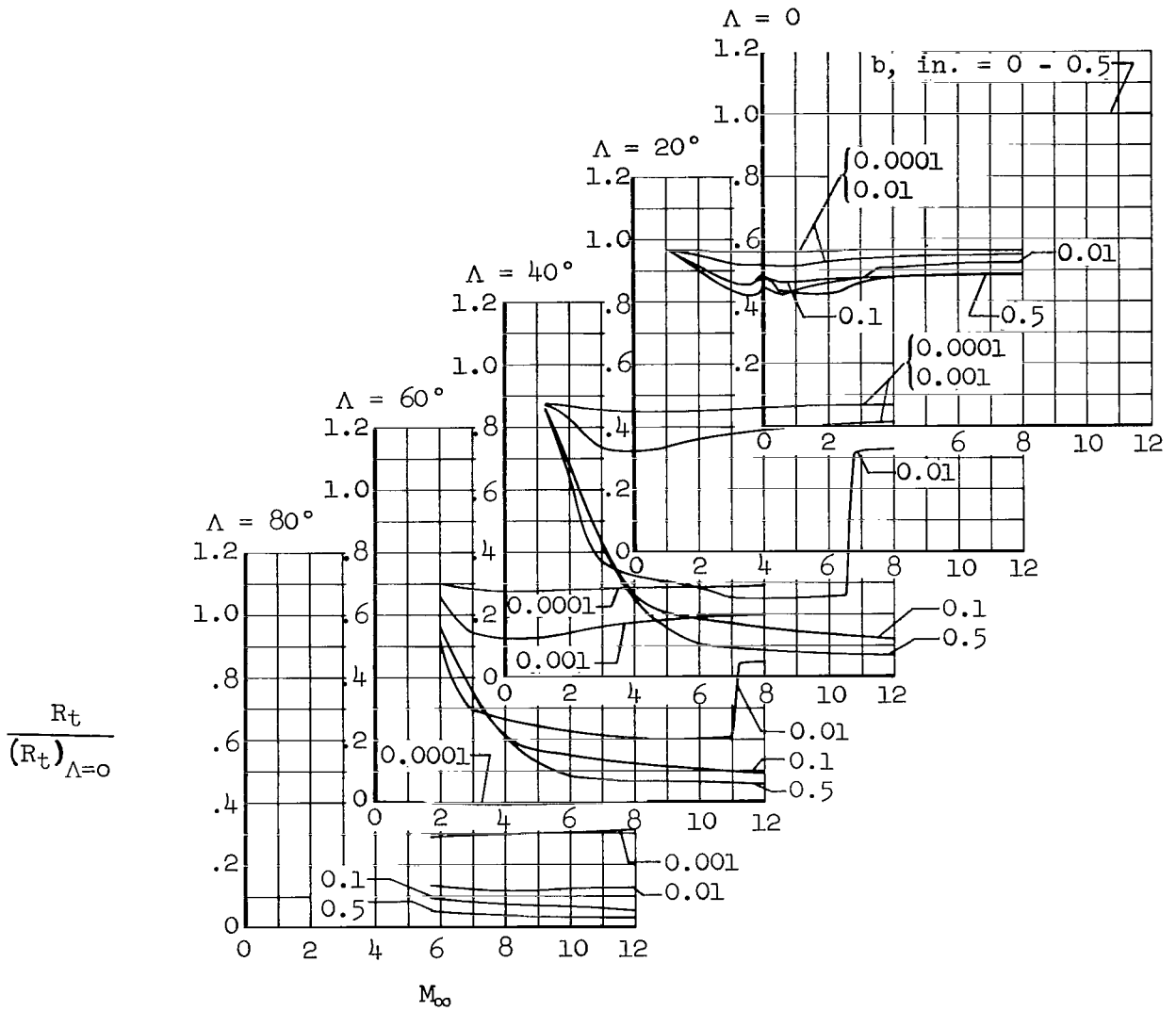


Chart 2.- Continued.



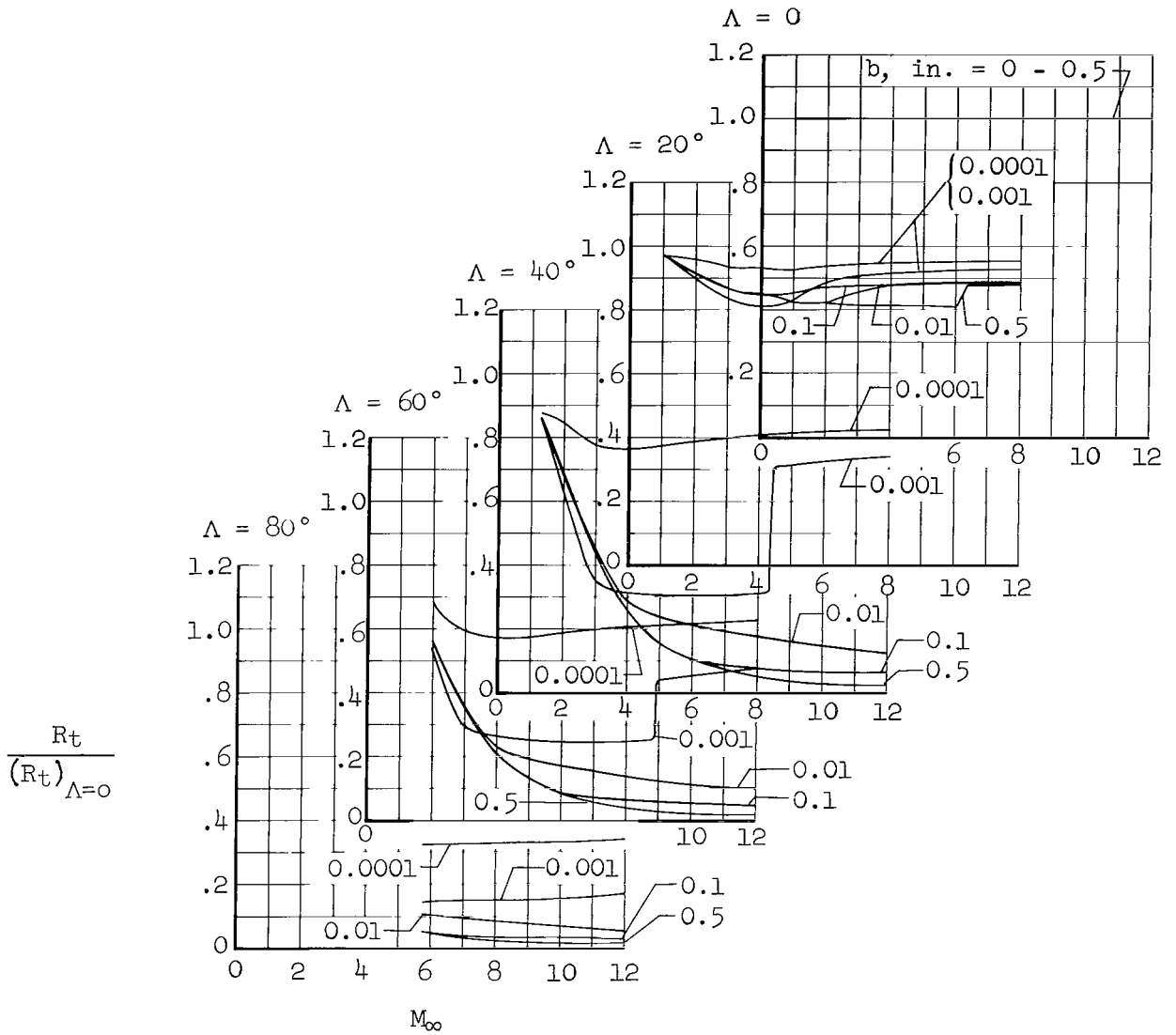
(c) $(R/\text{inch})_\infty = 10^5$

Chart 2.- Continued.



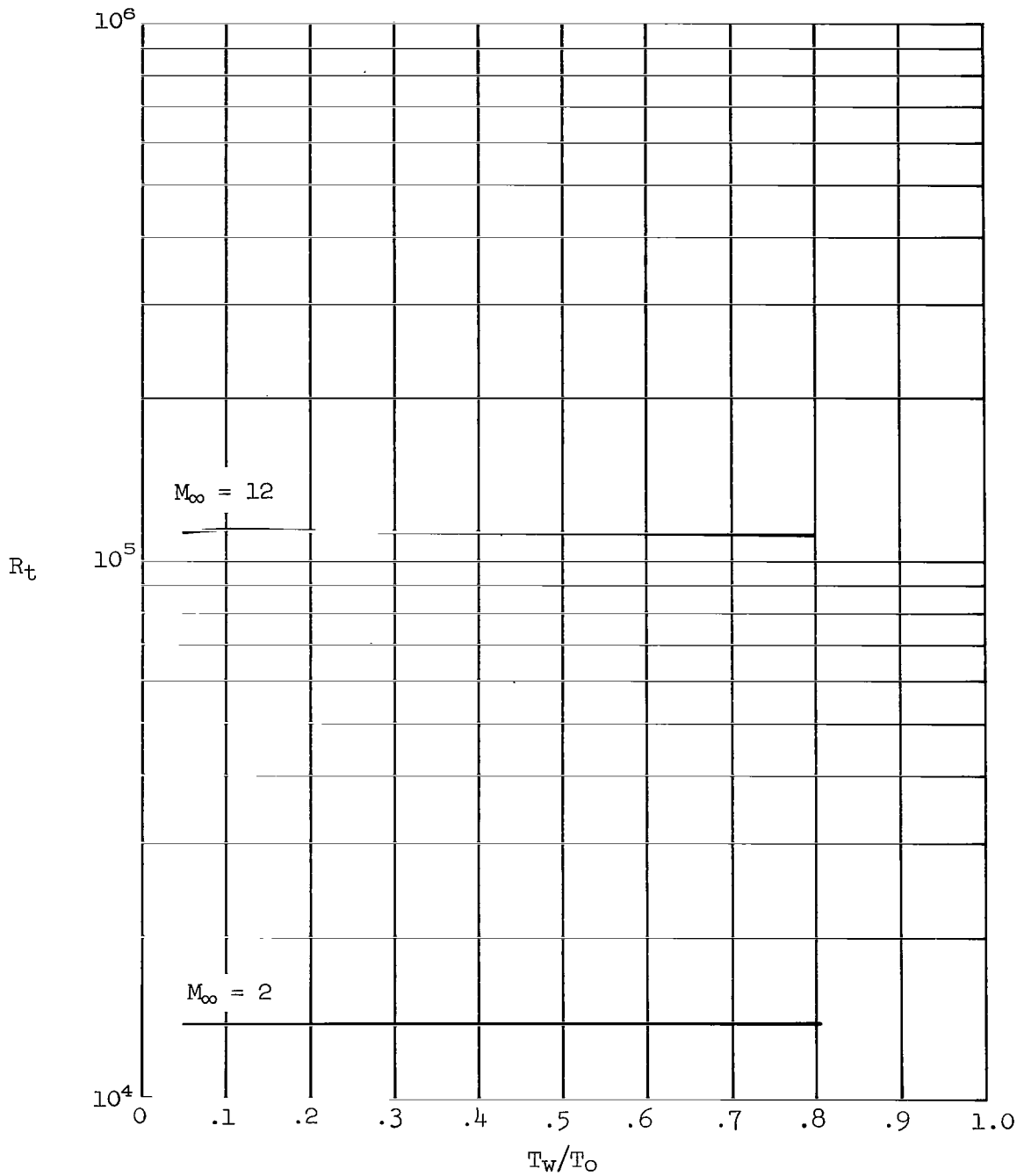
(d) $(R/\text{inch})_{\infty} = 10^6$

Chart 2.- Continued.



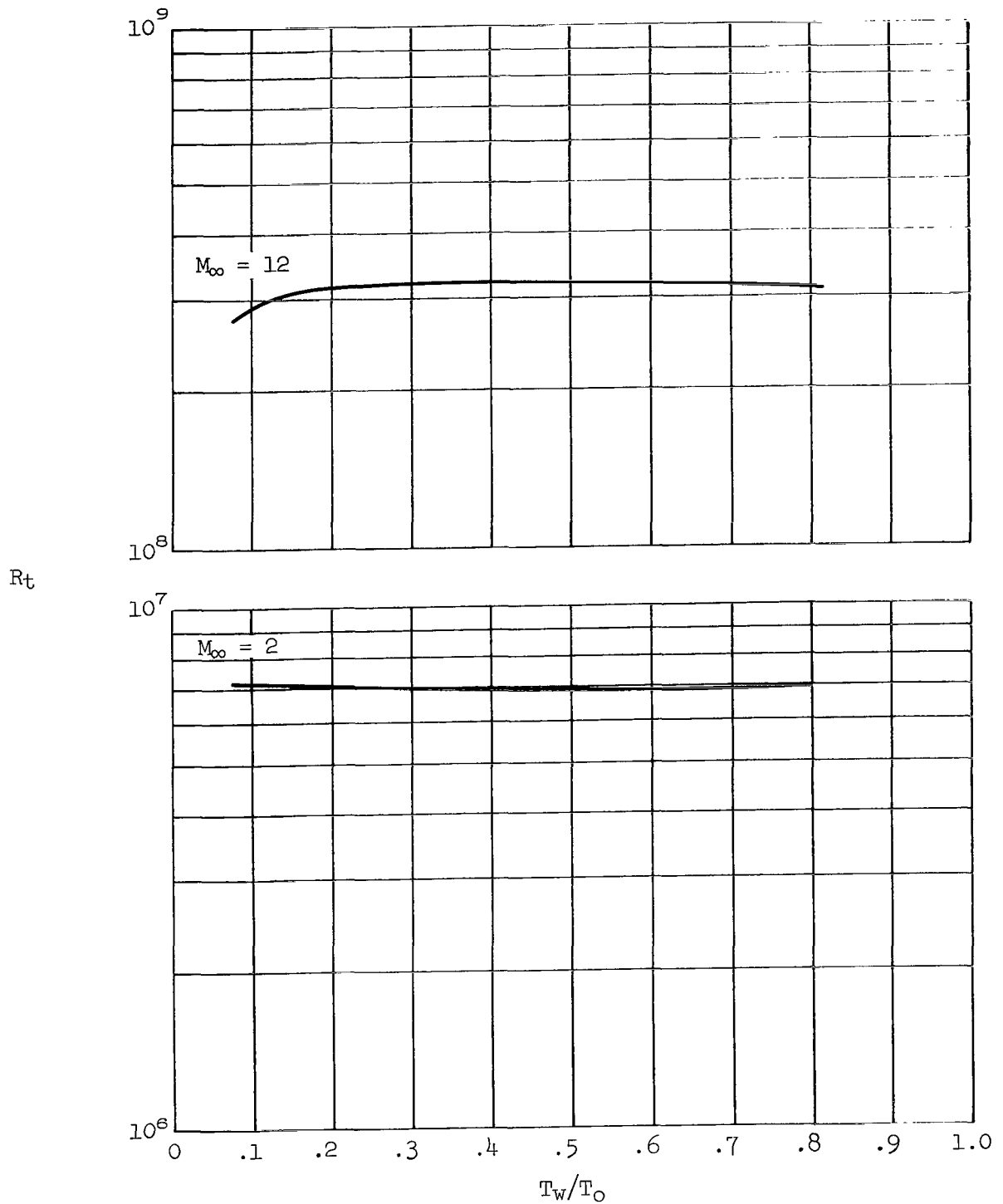
(e) $(R/\text{inch})_\infty = 10^7$

Chart 2.- Concluded.



(a) $(R/\text{inch})_\infty = 10^3$

Chart 3.- Estimated effect of wall-to-total temperature ratio on transition Reynolds number for a flat plate; $b = 0.01$ inch, $\Lambda = 0$, $T_w = 400^\circ$ R.



(b) $(R/\text{inch})_\infty = 10^7$

Chart 3.- Concluded.

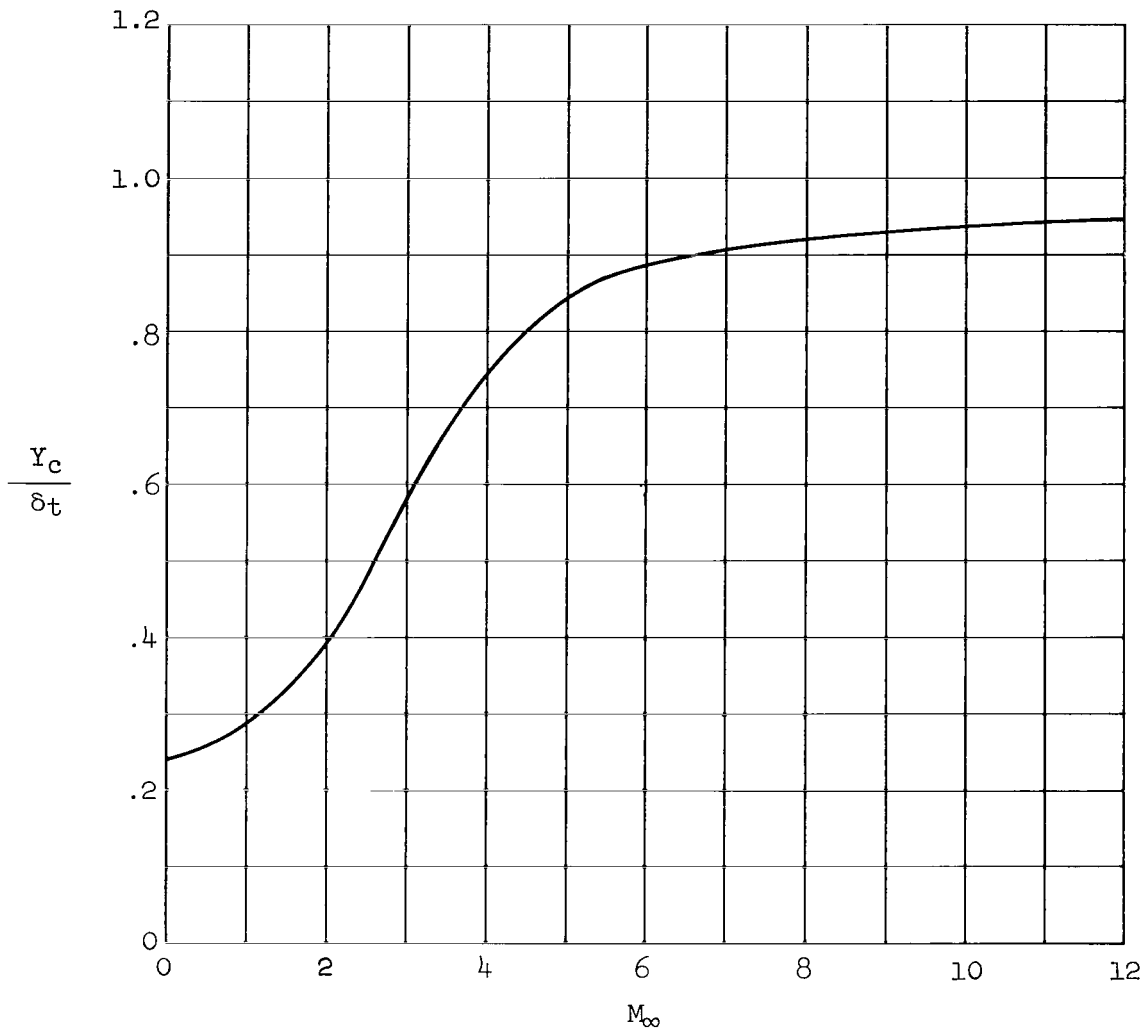


Chart 4.- Effect of Mach number on the critical height to boundary-layer thickness ratio from reference 1.

FIRST CLASS MAIL



POSTAGE AND FEES PAID
NATIONAL AERONAUTICS AND
SPACE ADMINISTRATION

020 001 37 51 305 70151 00903
AIR FORCE WEAPONS LABORATORY /WLOL/
KENTLAND AFB, NEW MEXICO 87117

ATLANTA, GEORGIA, OFFICE, U.S. AIR FORCE LIBRARY

POSTMASTER: If Undeliverable (Section 151
Postal Manual) Do Not Return

"The aeronautical and space activities of the United States shall be conducted so as to contribute . . . to the expansion of human knowledge of phenomena in the atmosphere and space. The Administration shall provide for the widest practicable and appropriate dissemination of information concerning its activities and the results thereof."

— NATIONAL AERONAUTICS AND SPACE ACT OF 1958

NASA SCIENTIFIC AND TECHNICAL PUBLICATIONS

TECHNICAL REPORTS: Scientific and technical information considered important, complete, and a lasting contribution to existing knowledge.

TECHNICAL NOTES: Information less broad in scope but nevertheless of importance as a contribution to existing knowledge.

TECHNICAL MEMORANDUMS: Information receiving limited distribution because of preliminary data, security classification, or other reasons.

CONTRACTOR REPORTS: Scientific and technical information generated under a NASA contract or grant and considered an important contribution to existing knowledge.

TECHNICAL TRANSLATIONS: Information published in a foreign language considered to merit NASA distribution in English.

SPECIAL PUBLICATIONS: Information derived from or of value to NASA activities. Publications include conference proceedings, monographs, data compilations, handbooks, sourcebooks, and special bibliographies.

TECHNOLOGY UTILIZATION PUBLICATIONS: Information on technology used by NASA that may be of particular interest in commercial and other non-aerospace applications. Publications include Tech Briefs, Technology Utilization Reports and Notes, and Technology Surveys.

Details on the availability of these publications may be obtained from:

**SCIENTIFIC AND TECHNICAL INFORMATION DIVISION
NATIONAL AERONAUTICS AND SPACE ADMINISTRATION
Washington, D.C. 20546**